

Calcium oxalate crystallization in synthetic urinary medium: the impact of a more complex solution medium, organic molecules and zinc ions

Odin Bottrill¹, Matthew Boon¹, Timothy Barker¹, Franca Jones^{1*}

1. Curtin Institute for Functional Molecules and Interfaces, School of Molecular and Life Sciences, Curtin University.

*Mail: Curtin University, GPO Box U1987, Perth, Australia 6845.

Email: F.Jones@curtin.edu.au Phone: 618 9266 7677

Abstract:

In this manuscript the impact of three organic molecules (in the presence and absence of zinc ions) in a more realistic solution medium is presented. The impact of the urinary medium on the morphology of the calcium oxalate monohydrate formed is similar to that seen in the presence of citric acid, the dominant component. The particles formed are relatively flat, rounded particles. In the presence of zinc ions, the particles are little changed with the main change being more rounded particles. The presence of the different organic acids show different impacts for different organics. Ethylenediaminetetraacetic acid complexes calcium ions and lowers the supersaturation as a chelator would be expected to. It also impacts the growing crystal changing the morphology. In the case of tartaric acid, adsorption onto critical nuclei and/or growth features leads to incorporation. Finally, the most complex impact was found for maleic acid. Maleic acid interacts with citric acid, inhibiting the citric acid effect. This can be seen in the morphology of particles being similar to those in pure water. The presence of zinc ions generally led to zeta potential values that were closer to zero and therefore would increase the propensity for these particles to coagulate.

Keywords: A1 Biocrystallization, A1 Crystal morphology, A1 Impurities, A1 Nucleation, A2 Growth from solutions, B1 Calcium compounds

Introduction:

Biom mineralization is an important and widespread process that occurs during everyday life with examples being bone,[1] teeth,[2] skeletal tissues in sponges,[3] crustaceans,[4] egg,[5] and mollusk shells.[6] By studying these natural systems “Biomimetic materials chemistry” aims to use the new found approaches for applications in material chemistry.[7] Therefore, crystal systems such as calcium carbonate, calcium oxalate and calcium phosphate are especially important due to their presence as biominerals in nature.[2,4,7] In Nature, calcium oxalate is abundant in many species of plants,[8,9] existing as a multitude of phases ranging from amorphous, to hydrated forms.[10,11,12]

However, not all biomineralization is desirable. In humans calcium oxalate is a biomineral with great medical significance, specifically regarding urolithiasis[13] and the formation of kidney stones.[14,15] This undesirable disease affects ~10% of the world’s population per generation[16] with an expected increase in the number of carriers for the foreseeable future. Calcium oxalate is vastly important in urolithiasis, as kidney stones consist of a mixture between calcium oxalate mono and di-hydrate forms (approximately 70%), with lower incorporations of calcium phosphate ~8.9%, uric acid ~ 10.1%, struvite ~9.3%, various organic materials ~0.8% and cystine ~0.7%.[17] The formation of kidney stones has been heavily

studied with multiple factors linked to its cause including dietary, environmental, genetic and urinary infection factors.[14] Kidney stones are formed as a combination of ionic and organic components which aggregate as crystals within urine and epithelial cells.[18] A tear in a tube can act as an aggregation site for the crystals to form, which results in a blockage occurring. Organic macromolecules such as lipids, polysaccharides and proteins, which exist as in the organic matrix interlaced throughout kidney stones, are hypothesised to control of kidney stone formation either inhibiting or promoting crystallisation or aggregation .[15] Despite this, very few treatment options exist for sufferers. While recent studies investigated a wide range of compounds from macromolecules[15,19] to single inorganic ions[7,20,21], alkali metals[19] etc., most of these studies are in pure water systems, or at unrealistic pHs.

The aims of this work are twofold:

- (i) Firstly, expand on our previous work in pure water [22] to test promising additives in a more realistic environment. To do this, a synthetic urine was used as a growth medium for the calcium oxalate crystallization in this study. Synthetic urines have been used in the medical field over many decades, with numerous recipe variations being published with varying degrees of complexity.[23] The majority of the artificial urines published in the literature are at a physiological pH of 7. The synthetic urinary medium (SUM) used in this study was adapted from Brown *et al.*[24] as initial starting conditions for COM crystallization (see **Table 1** for final composition).
- (ii) Determine how the presence of zinc influences these additives.

The organic species investigated within this study were chosen based on previous work in pure water [22] and compared these to a molecule known to complex calcium. That is, tartaric acid and maleic acid were chosen due to promising results reported in Barker *et al.*[22] and ethylenediamine tetraacetic acid (EDTA) was chosen as it is a well-known chelator. Zinc ions were also a focus of this study, as

- (i) little data is available on the ion although it has been suggested that zinc ions are a moderately good inhibitor within aqueous medium of both calcium oxalate and phosphate crystallization.[25]
- (ii) Zinc ions have been implicated in the process of COM pathogenesis by promoting aggregation[26]

Zinc ions have a weak tendency for incorporation within calcium oxalate minerals with preferred formation of a zinc oxalate species.[27]

In this work, the impacts of the additives were assessed through their effects on morphology, nucleation and zeta potential.

Within kidney stones two hydrate forms are most common, referred to as whewellite and weddellite. The most thermodynamically stable phase, whewellite, also known as calcium oxalate monohydrate (COM, $\text{CaC}_2\text{O}_4 \cdot \text{H}_2\text{O}$) has a monoclinic structure.[28] Weddellite is the metastable form at room temperature, known as calcium oxalate dihydrate (COD, $\text{CaC}_2\text{O}_4 \cdot (2+x)\text{H}_2\text{O}$; $x \leq 0.5$), and is tetragonal in structure.[28] A third hydrate form also exists, calcium oxalate trihydrate (COT, $\text{CaC}_2\text{O}_4 \cdot (3-x)\text{H}_2\text{O}$; $x < 0.5$) however due to the thermodynamic instability, it is rarely observed within urinary media.[12] The expected morphology of COM is as a twin, either the contact and penetration twins (**figure 1, b,c**). In addition, the expected morphology in the presence of citric acid is shown as the SUM used in this work contains citric acid (**figure 1, d**). Comparisons to this expected morphology can then give information as to whether the additive prefers a particular face to adsorb on.

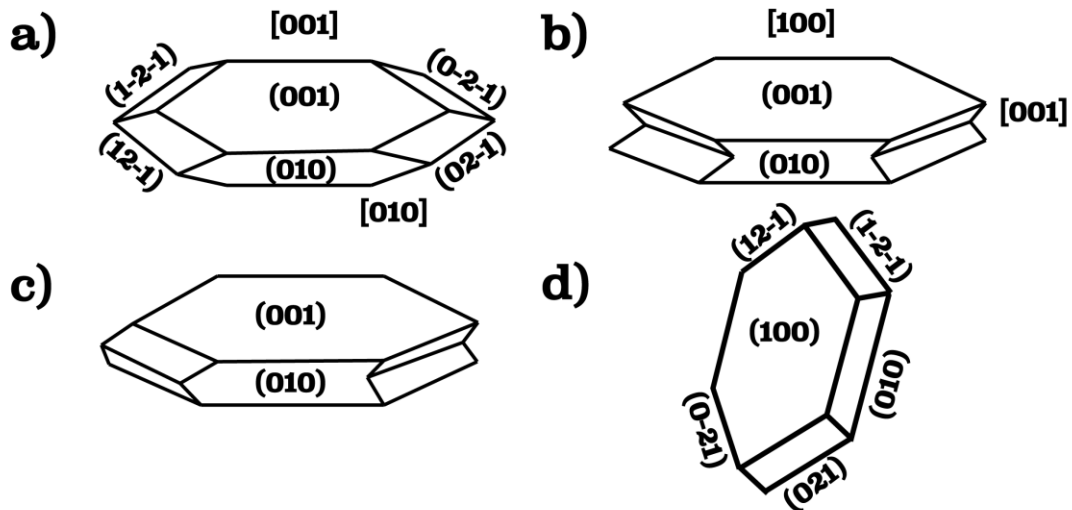


Figure 1) COM morphology a) single crystal[22] b) contact twin[29] c) penetration twin[30] d) expected morphology in the presence of citric acid

Materials and Methods:

All reagents used in these experiments were of analytical grade quality and used as received. The water used in all these experiments and stock solutions was ultrapure water (>18 MΩ resistance). All experiments were repeated ≥ 2 times and the average data is presented here.

A synthetic urinary medium (SUM) was modified from that reported in *Brown et al.*[24] (**Table 1**). A stock solution was prepared at 10 times the concentration and adjusted to a pH of 6.5 with hydrochloric acid. Potassium phosphate monobasic was stored separately to avoid phosphate precipitation occurring in the SUM. To avoid bacterial growth in the SUM, sodium azide (1% w/w) was also added.

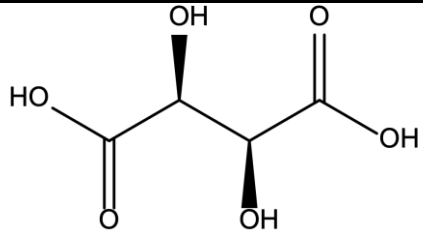
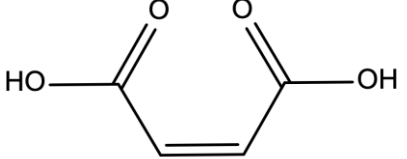
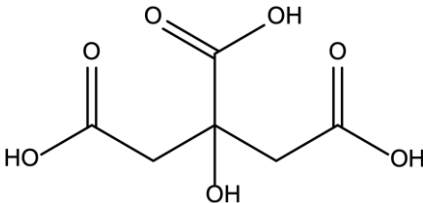
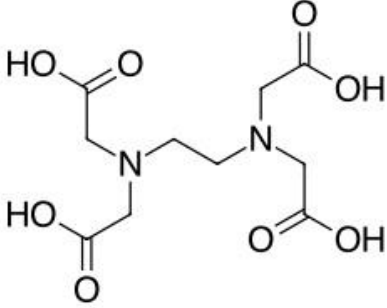
Table 1) Synthetic urinary medium (SUM) adapted from *Brown et al.*[24]

Species	Concentration (mM)
Sodium Chloride	105.50
Potassium Chloride	63.70
Ammonium Chloride	27.60
Magnesium Sulfate	3.95
Potassium Phosphate Monobasic*	3.23
Sodium Citrate	3.21

* kept separate from other SUM species

A total of 3 inhibitors were studied in both pure water and SUM environments. Each of the organic inhibitors investigated contained at least one carboxylic acid functional group (**Table 2**). Zinc chloride ($ZnCl_2$) was also investigated (held constant at 1 mM) as it is known to impact the formation of $CaOx$ and is linked to oxalate aggregation.[26,31] The concentration chosen is within the normal range found biologically.[32,33]

Table 2) List of organic compounds tested in SUM

Name	Molecular Weight	Structure
D-Tartaric Acid (TA)	150.09	
Cis-Maleic Acid (MA)	116.07	
Citric Acid (CA)	192.12	
Ethylenediaminetetraacetic Acid (EDTA)	292.24	

Bulk crystallization experiments in SUM:

The control experiments were conducted at a working pH 6.5 and a temperature of 37°C. A clean glass cover slide was placed into a pre-cleaned glass vial, then water, SUM stock solution (2 mL), phosphate monobasic stock solution (2 mL) and the calcium chloride (0.40 mM) were combined before equilibrating at 37 °C for 15 minutes. Sodium oxalate (0.40 mM) was added to initiate the crystallization reaction and the vial was left in a water bath at 37 °C for 18- 24 hours before removing the glass slide, which was rinsed with ultrapure water and dried.

The impact of the organic inhibitor was assessed both with and without zinc ions being present. The concentration of the organic inhibitor without zinc ions present was investigated at 20 mM while in the presence of zinc ions it was 10, 5 and 1 mM. The concentration of zinc ions was always 1 mM. The inhibitors were added after the calcium chloride and left to equilibrate to 37 °C in a water bath for 15 minutes before the addition of the oxalate solution. After the addition of the oxalate solution the samples were left in the water bath at 37 °C for 18-24 hours before the cover slide was removed, washed with water, dried and stored for further analysis. The area of the particles were calculated using ImageJ, by measuring the length and width of the (100) face of the crystals and multiplying them together. It should be noted that this is a slight overestimation of the true area due to the assumption of a 'perfect' rectangle. The form of

calcium oxalate (mono, di, tri-hydrate etc.) was confirmed through Raman spectroscopy using the WITec alpha 300SAR.

Confocal Raman and Optical Analysis:

Optical images and confocal Raman spectra were collected using the WITec alpha 300SAR, utilising a frequency-doubled NdYAG laser of wavelength 532 nm (green) and of 50 mW power using silicon as the reference material. Single point spectrums were conducted using 100 accumulations at 0.1 second integration time. Depth analysis was performed on particles at a depth of 10 μm with 10 accumulations at 0.05 second integration. The resulting spectra were processed using WITec Project Four® software.

Scanning electron microscopy (SEM):

Once the cover slides were analysed using optical and Raman analysis, they were mounted onto an SEM stub using double-sided carbon tabs with liquid graphene being applied to the edge of the samples to limit the impact of charging. The samples were then coated in platinum (~4 nm) and analysed using a Neon FIB-SEM. The resulting SEM images were then processed using ImageJ to obtain information regarding the particle area.

Dynamic Light Scattering (DLS):

DLS was used to determine the nucleation behaviour of the crystallization systems. A Malvern Zetasizer Nano-ZS was used to collect particle counts versus time. The concentrations investigated using DLS were identical to the concentrations used in the bulk crystallization experiments. In a Teflon beaker the water, calcium chloride, SUM stock solution and organic additive (if required) were combined and stirred constantly at 400 rpm. An aliquot was withdrawn from this solution approximately every 3 minutes into a disposable cuvette and measurements were recorded using an integration time of 10 seconds with 10 measurements being recorded for the first 20 minutes.

Results and Discussion:

Morphology:

In the presence of the SUM, calcium oxalate monohydrate (COM) was formed as was found in pure water. The main difference between the particles formed in pure water compared to SUM was that penetration twinning was significantly reduced. The morphology of the COM formed within the SUM (**Figure 2, c**) differs to that previously reported in pure water (**Figure 2, a**). The SUM COMs morphology has more rounded edges, through the inhibition of the (100), (021) and (121) faces, which results in a more circular morphology. This is due to the presence of CA being present in SUM which is a well-known inhibitor of CaOx[1,34].

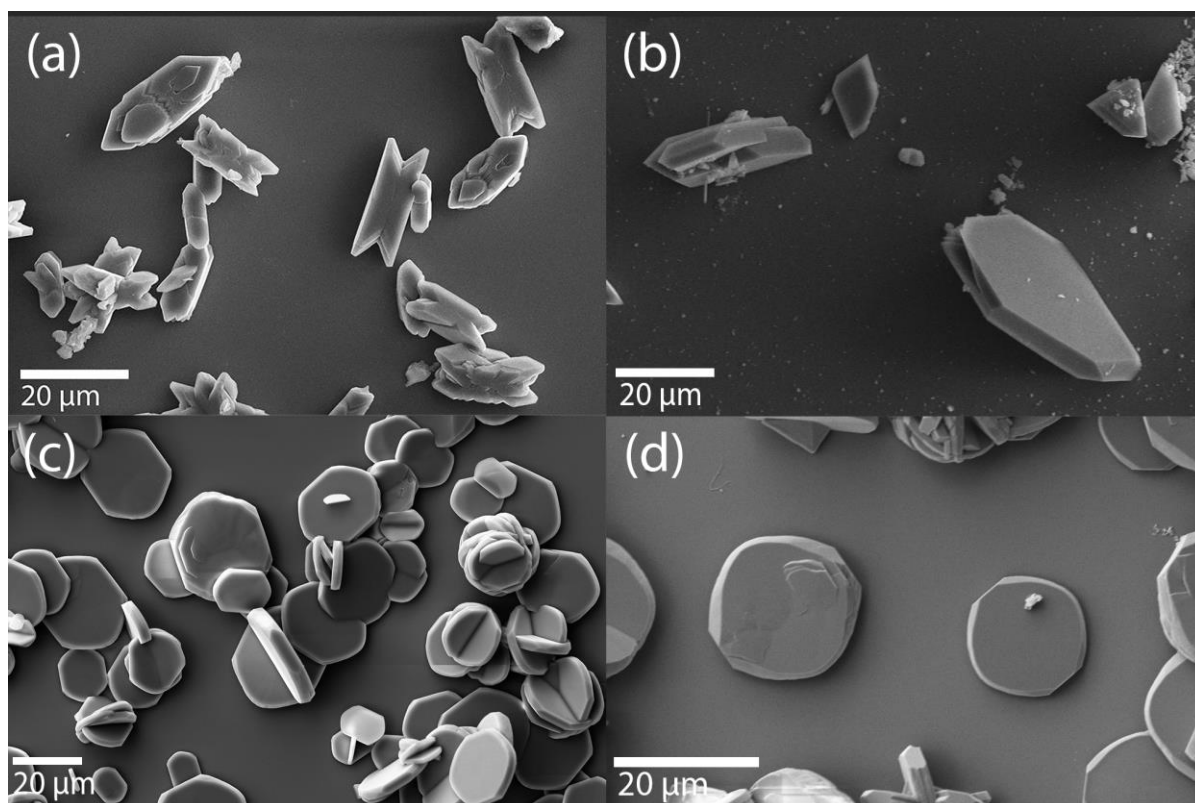


Figure 2) SEM images of COM formed in (a) pure water (b) pure water + zinc ions (20mM) reproduced with permission from Barker *et. Al* [22] (c) SUM without zinc ions and (d) SUM with zinc ions (1 mM)

The presence of zinc ions in pure water had a more dramatic impact on morphology than in SUM but this is related to the concentration of Zn^{2+} ions present in these two cases (20mM c/f 1mM) (**Figure 2, c**). The effect at low concentration is not significant (**SupFig 1**). In the presence of Zn^{2+} and SUM, it is the same (100), (021) and (121) faces that are inhibited but to a greater degree, resulting in smaller (010) faces and rounder particles overall (**Figure 2, d**).

Tartaric acid in pure water showed a significant impact on particle size (**Figure 3, a**) but this impact disappeared when zinc ions were also present (**Figure 3, b**). The particles returned to control-like morphologies and sizes when $TA+Zn^{2+}$ was present. The main impact of tartaric acid on the morphology of the COM formed in SUM was the smaller size (compared to SUM alone) but thicker COM crystals formed (**Figure 3, c**). The (010) faces appear more dominant when compared to the SUM COM (**Figure 2, c**). Compared to the control COM particles formed in SUM, those formed in the presence of TA were also more rounded.

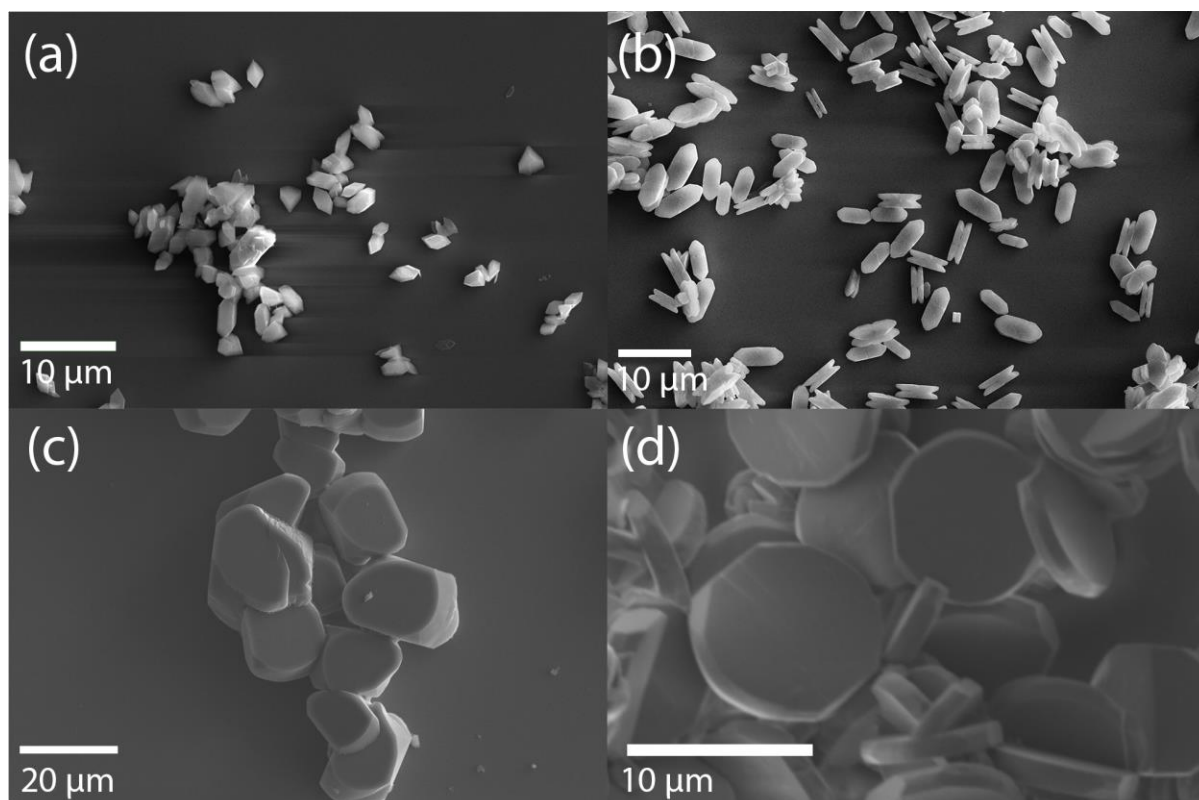


Figure 3) SEM images of COM formed in the presence of a) tartaric acid (TA) in pure water b) TA+Zn²⁺ (1mM) in pure water reproduced with permission from Barker *et. al*[22] c) TA in SUM and d) TA+Zn²⁺ (1mM) in SUM

Incorporating both the zinc ions and TA into the SUM showed larger COM particles when compared to the absence of zinc ions. In addition, the particles in SUM formed in the presence of TA + Zn²⁺ are thinner than TA alone, suggesting a relative slower growth in the *a*-axis. The presence of both TA and Zn²⁺ showed the possible presence of small (001) faces (**Figure 3, d**). As found in the case of pure water, the presence of zinc ions appears to limit the impact of the tartaric acid.

The COM grown in the presence of maleic acid in SUM takes on an elongated hexagonal morphology similar to that of COM formed in pure water (**Figure 4, c**) but larger. For the morphology to return to the morphology of COM in pure systems (**Figure 4, a**), suggests that the presence of maleic acid prevents interaction between the CaOx and citric acid. These results suggests a competitive interaction between CA and MA either in solution or on the surface of COM particles (or both).

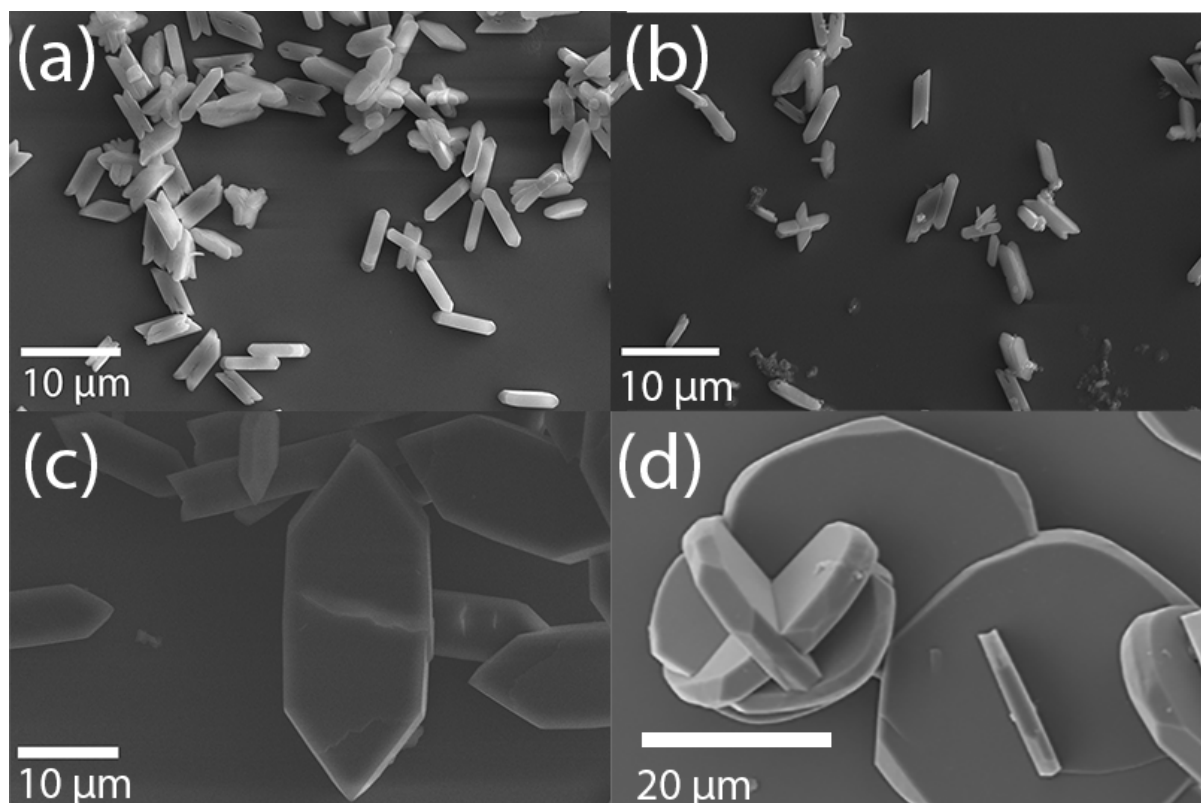


Figure 4) SEM images of COM formed in the presence of a) maleic acid (MA) in pure water b) MA+Zn²⁺ (1 mM) in pure water reproduced with permission from Barker *et. al*[22]. c) MA in SUM and d) MA+Zn²⁺ (1 mM) in SUM

The addition of zinc ions into the system shows little impact when in pure water (**Figure 4, b**) but in SUM the morphology of the COM particles revert back to the morphology observed in SUM alone (**Figure 4, d**). This implies that the zinc ions are interacting with the MA in the SUM solution, removing it from competing with the CA and allowing the morphology to revert back to the SUM grown COM.

EDTA formed in the presence of water at a low concentration (1 mM) showed particles similar to COM grown in pure water (**SupFig 2**) but blockier and larger. Incorporation of Zn²⁺ ions into the EDTA in pure water resulted in complete inhibition of the COM. The morphology of COM in the presence of EDTA is shown in **Figure 5a**. This morphology also appears to show a large amount of aggregation, with crystals growing into other crystals. The (010) face has almost disappeared, and the particles are dominated by the (12-1) and (021) faces. The width of the particles in the presence of EDTA is similar to the COM particles formed in SUM but their lengths are much smaller. The morphology is significantly different to that of the citric acid impacted crystals, which suggests that the EDTA is causing significant inhibition in the crystal growth process. The morphology of the CaOx when both the EDTA and Zn²⁺ ions (**Figure 5, b**) into the growth solution shows a morphology similar to the MA+Zn²⁺ (**Figure 4, d**). This is due to the binding coefficient of EDTA is greater with the Zn²⁺ ions than with the Ca²⁺ (**Table 4**) allowing for CA to predominately influence the growth of the COM.

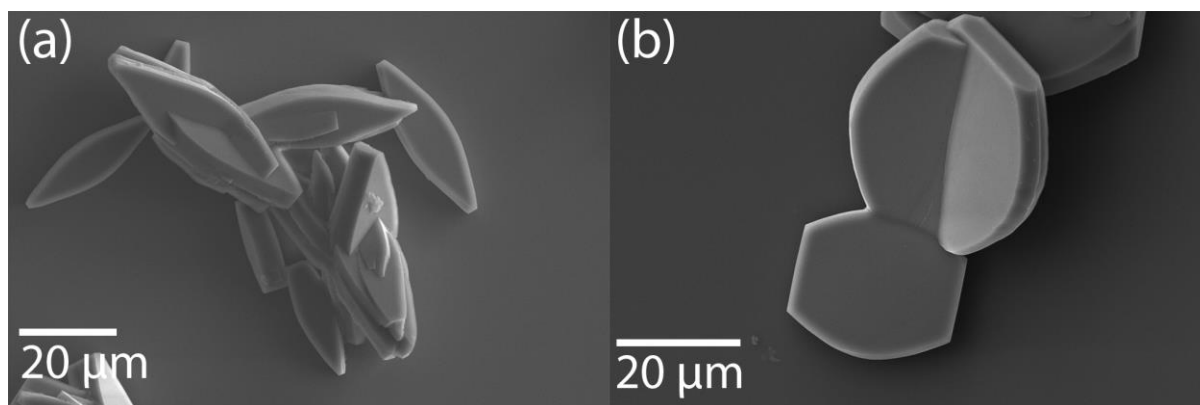


Figure 5) SEM images of COM formed in SUM in the presence of Ethylenediaminetetraacetic acid (EDTA) (left) and EDTA+Zn²⁺ (right)

Using ImageJ software the crude area of the particles in the presence of the SUM and additives were calculated by measuring the length of the (100) face and multiplying it by the width of the (100) face (**Table 3**). The area of the SUM grown particles both with and without Zn²⁺ ions present showed particles of half the area. This could be due to the present of the CA acting as a weak inhibitor of the COM and allowing for a templating control over the COM.

The impact of both TA and MA had on the crude area of the (100) faces was a reduction to approximately half to a third of the control values. While the EDTA has approximately the same size area of crystals despite the dramatic morphological difference when the EDTA is present (**Table 3**).

Table 3) Area data for COM grown within the SUM and respective organic with and without zinc ions.

Additives (20 mM)	SUM		Water	
	Area of COM <i>without</i> Zn ²⁺ being present (μm ²)	Area of COM <i>with</i> Zn ²⁺ being present (μm ²)	Area of COM <i>without</i> Zn ²⁺ being present (μm ²)	Area of COM <i>with</i> Zn ²⁺ being present (μm ²)
None	-	-	20.8±4.7	692±91
Citric Acid (CA)	-	-	43.4±4.6	11.3±2.3
Synthetic Urine Medium (SUM)	672±90	391±48	-	-
Tartaric Acid (TA)	207±38	62±13	7.1± 1.7	11.27±2.7
Maleic Acid (MA)	272±72	999±222	10.7±2.3	7.44±1.4
Ethylenediaminetetraacetic Acid (EDTA, 1 mM)	647±104	1771±423	245±63	-

Incorporating the Zn^{2+} ions into the growth solutions has an impact in all four systems. In the presence of the SUM with no additives, the area drops to two thirds the area of the pure SUM. For TA and Zn^{2+} the area of the crystals is dropped to 10% the area of the SUM crystals. This can be due to the Zn^{2+} ions not preferentially binding to either the TA or the CA within the system allowing for both acids and Zn^{2+} ions to impact the growth of the COM. For both the MA and EDTA systems, with the Zn^{2+} ions are present, a significant increase in the area of the COM is observed, 370% and 270% respectively.

Raman analysis:

Confocal Raman can be used to probe the interior of the COM crystals formed. **Figure 6** shows how the instrument can collect Raman spectra at different depths as well as different x,y positions to give information about whether the organic is incorporated. This can be done in two ways depending on the system under investigation –

- (i) The fluorescence due to the organic molecule can be taken as a proxy to concentration (if no other species fluoresces)
- (ii) Bands known to be due to the organic species can be interrogated to see where they occur and the intensity measured can be converted to a ‘heat map’ to visually show where the highest intensity for the peak of interest is.

The COM that was grown within the SUM all exhibited a degree of fluorescence due to the presence of the CA within the SUM. Thus, method (i) could not be used in this instance.

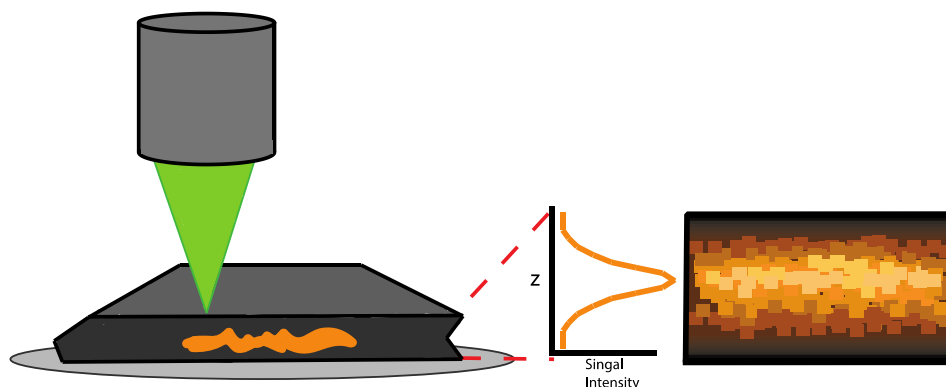


Figure 6. As the focal depth of the Raman laser changes within the crystal, the intensity of the desired peak can be monitored and plotted with respect to the ‘height’ (z-value) or with respect to the x,y position at a fixed z-value

While this experiment was completed for all the organics investigated in this work, only in the case of TA were peaks observed that were different to the control COM formed in SUM. When TA is present in the SUM two bands, 2500 cm^{-1} and 2700 cm^{-1} , become apparent; these bands can be attributed to the presence of the TA. Confocal Raman depth analysis of the COM grown in the presence of the TA (and TA+ Zn^{2+}) shows a localized concentration of TA (**SupFig 3** and **Figure 7** respectively) in the centre of the particle. Given this result, it is surprising that the presence of zinc ions and TA do not have such a significant impact on morphology. This could be due to the TA+ Zn^{2+} impacting all faces to a similar degree rather than specific faces. The confocal Raman also shows the probable contact twinning plane as the depleted region between them. In any case, this result suggests that the TA is active and incorporated during the early stages of crystal formation/growth. It is also possible that since this is a batch system, the TA adsorbs strongly and incorporates early on when concentration is highest and as the concentration is diminished less is available to incorporate at later stages.

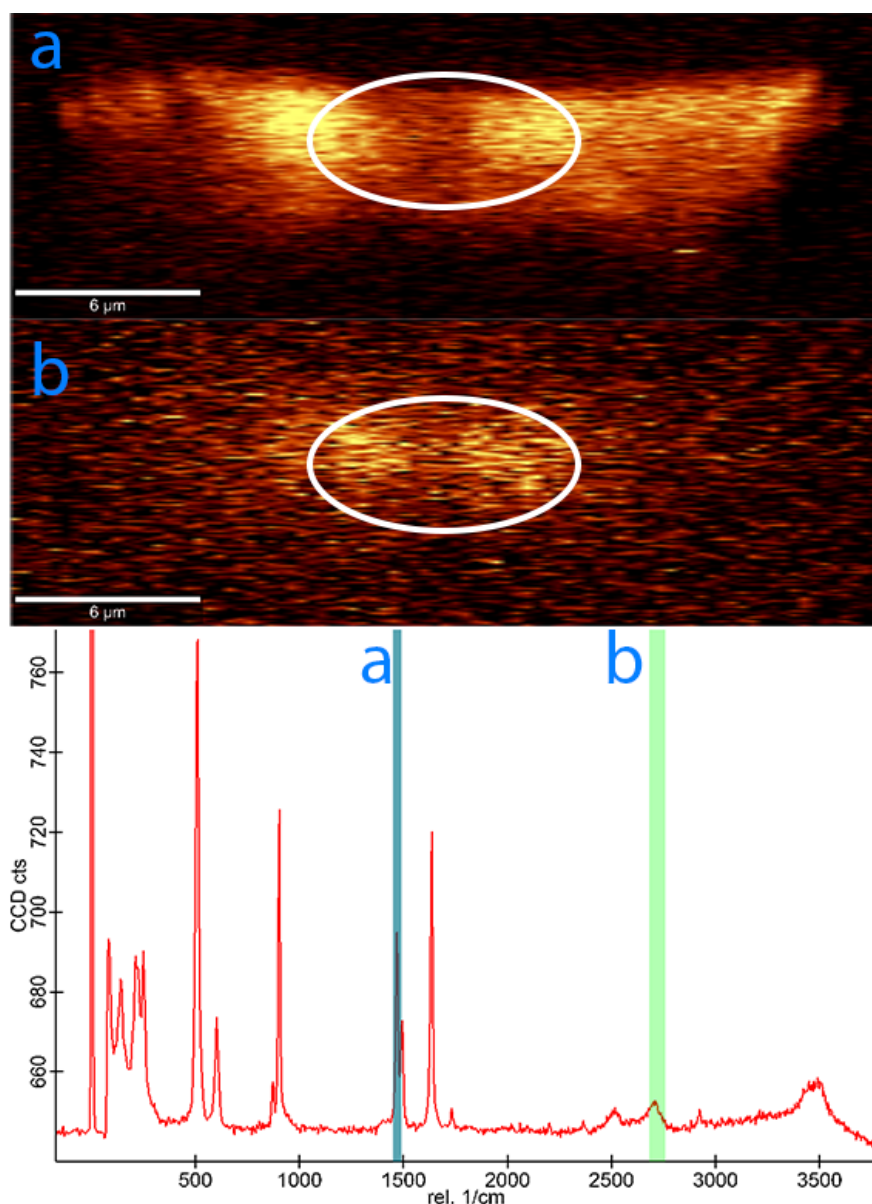


Figure 7) Confocal Raman heat map of COM grown in the presence of SUM, TA + Zn²⁺ (**A**) the COM 1490 cm⁻¹ signal and (**B**) the COM 2700 cm⁻¹ signal as shown in the spectrum

Due to the incorporation of the TA, the TA must be acting as a strong inhibitor on the initially formed COM. However, this is different to the behavior of the TA in pure water where it was found to adsorb weakly onto the surface of the COM with little TA being detected within the resulting crystal.

From these results we see that tartaric acid in pure water is weakly interacting with COM mainly through surface interactions while in SUM the tartaric acid is strongly adsorbing to the point of being incorporated.

Dynamic Light Scattering (DLS) Analysis:

It should be noted that the concentrations of calcium and oxalate ions in pure water and SUM differ. This is because the presence of the other species impacts the solubility of COM in solution. However, due to not being able to calculate the saturation index in SUM it is also

unknown whether these different systems (pure water and SUM) are at a similar supersaturation

Dynamic light scattering (DLS) was used to determine the effect additives have on the homogeneous nucleation behaviour of calcium oxalate. Firstly, it is possible to establish whether the nucleation rate was amplified or reduced in the presence of each organic additive (i.e. determine the impact on the particle count or the onset of nucleation). Secondly, it is possible to determine the impact zinc ions have on nucleation and how this changes with the addition of organics. The typical nucleation graph (**Figure 8**) is shown by the control data of calcium oxalate in the absence of any additives at pH 7. This shows an increase in the derived count rate, indicating nucleation is occurring through an increase in particle numbers, before eventually plateauing. The plateau, in essence, shows that there are no further nucleation events occurring (but crystal growth can continue). Aggregation and/or settling can result in the counts decreasing at longer time periods.

Figure 8 compares the nucleation behaviour of COM in pure water and in SUM with and without the presence of zinc ions. In pure water the nucleation of CaOx occurs quickly and a stabilisation in particle numbers is also reached quickly. In contrast, the CaOx grown in the SUM shows an increase in the number of counts over the first 5 minutes, to a maximum which is almost $\frac{1}{4}$ of that in pure water. Aggregation and/or settling is also more significant when SUM is present, with a small but steady decrease in the number of counts after the maximum. As stated above, this may be due to differences in supersaturation given that the SUM will impact the solubility of calcium oxalate solids. The presence of zinc ions results in a decrease in the overall number of counts detected irrespective of the system.[22] The impact of Zn^{2+} in SUM appears to be significantly inhibit nucleation with fewer counts being observed than the control SUM maximum counts of ~ 5000 kcps (**Figure 8, circles, bottom**). There appears to be a slightly longer induction time in this case before there is a rise in counts is observed, at around 10 minutes. The final counts for the SUM + Zn^{2+} case at the end of the measurements are under half that of the SUM maximum (**Figure 8, diamonds, bottom**).

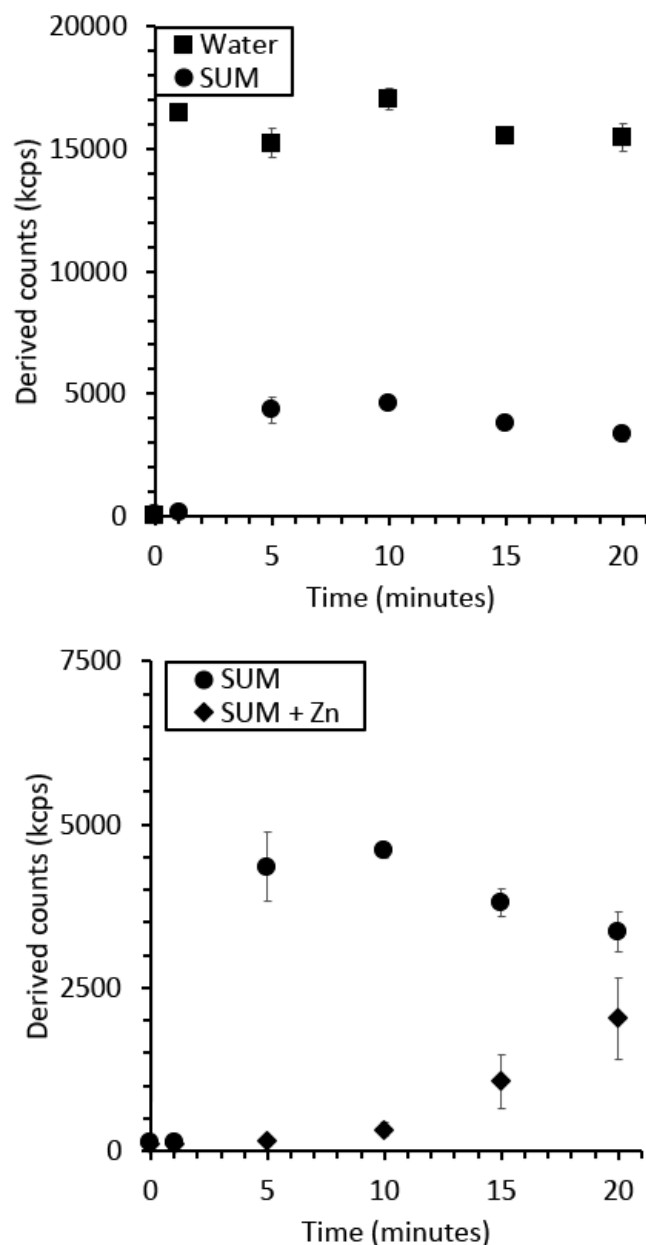


Figure 8) Dynamic light scattering plots of the derived counts of CaOx grown in the presence of water (**squares, top**), SUM (**circles**) and SUM with zinc (**diamonds, bottom**)

The decrease in counts due to the presence of zinc ions can be attributed to the zinc ions interacting preferentially with the oxalate. The binding coefficients obtained from the JESS database[35] suggest oxalate will bind to the Zn^{2+} over Ca^{2+} (see **Table 4**) if there is no other competition. The oxalate binding to Zn^{2+} reduces the nucleation due to the lowering of the oxalate activity.

Table 4) Complexation constant data for ion pairs obtained from the JESS database[35]

Positive Ion	Number of deprotonated carboxylic acid groups	lnK Value				
		CA	TA	MA	EDTA	Oxalate
Zn²⁺	4	-	-	-	14.61	-
	3	4.55	-	-	9.00	-
	2	2.96	2.6	2.19	NA	4.1
	1	1.71	1.44	NA	NA	1.72
Ca²⁺	4	-	-	-	9.36	-
	3	1.80	-	-	3.4	-
	2	1.83	1.8	2.55	NA	2.36
	1	1.1	1.11	NA	NA	1.38

NA = not available

- Not applicable

The impact of TA on the nucleation of CaOx within SUM shows significant inhibition of nucleation (**Figure 9, top**), similar to the case in pure water (see **SupFig 4.**). Little nucleation appears to occur over the first 20 minutes. The rate of formation of particles is lower than that of the addition of zinc ions to SUM (**Figure 9, bottom**). TA is not expected to significantly complex with either Zn²⁺ or Ca²⁺ (see Table 4) suggesting that TA therefore acts as a threshold inhibitor. A threshold inhibitor is one that does not act by chelation but impacts at very low concentrations through adsorption onto critical nuclei or to growth features (such as kinks and steps).[36] In the presence of TA+Zn²⁺ in SUM the nucleation behaviour does not significantly alter, unlike the case in pure water (see **SupFig 5**). Interestingly, the ability of TA to still inhibit nucleation significantly in the presence of Zn²⁺ (**Figure 9, green**) supports the confocal Raman results presented above (**Figure 7**). Thus, inhibition in SUM when TA and Zn²⁺ are present is due to strong interactions between TA and COM but as suggested above this must be less face-specific.

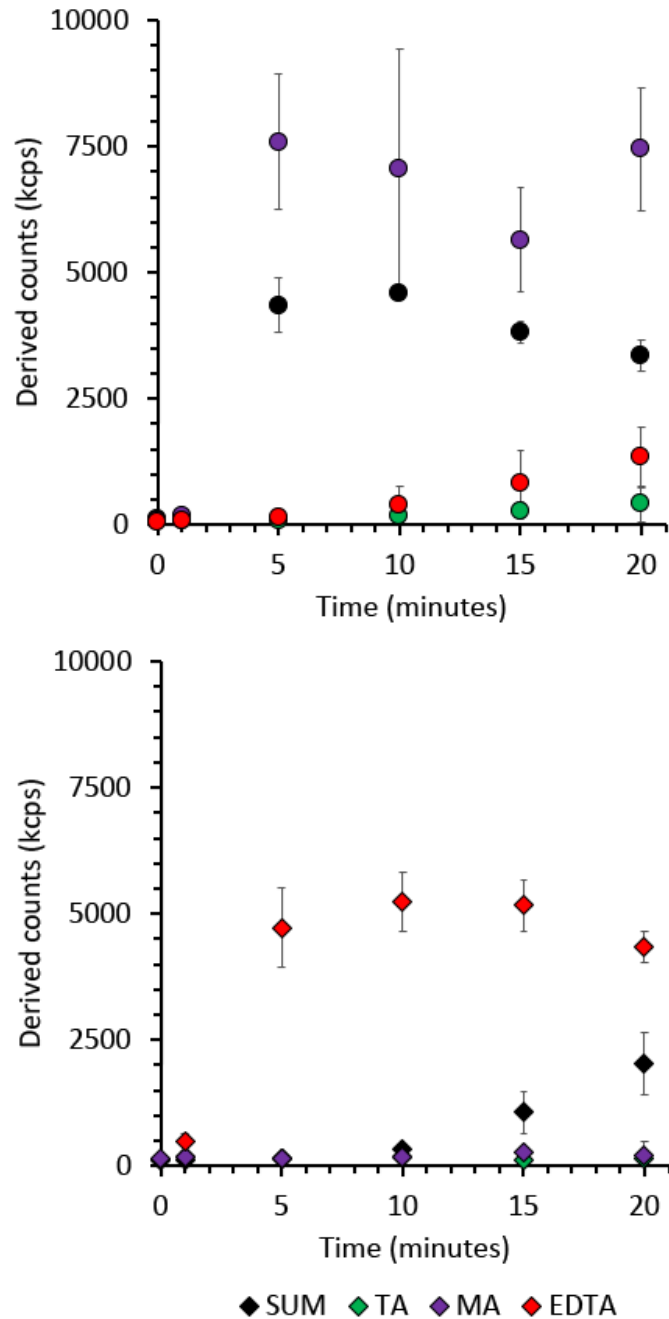


Figure 9) Dynamic light scattering plots of the derived counts of CaOx grown in the presence of SUM (**TOP**) and SUM with Zn²⁺ (**BOTTOM**) with the control (**black**) and TA (**Green**), MA (**Purple**), and EDTA (**Red**)

Maleic acid only showed minor inhibition of nucleation in pure water (see **SupFig 4**) while there appears to be a slight increase in nucleation rate in SUM (**Figure 9, purple**). In the presence of zinc ions, MA significantly inhibits nucleation in SUM while is similar to the control in pure water. Combined with the morphology results, it can be assumed that the interaction of MA with citric acid is disturbed by the presence of Zn²⁺. In addition, this system is able to impact nucleation more so than SUM + Zn²⁺, suggesting there is an additional impact. However, maleic acid is not expected to complex zinc ions in preference to calcium ions according to Table 4. In combination with the previous results it is clear that MA impedes CA's ability to inhibit but when zinc ions are present the CA is able to impact morphology once

again. The fact that the nucleation rate is even lower than SUM + Zn²⁺ is hypothesised to be due to MA being able to also inhibit (through adsorption onto nuclei and changing the surface free energy) rather than interacting with CA in solution.

The presence of EDTA in SUM also resulted in significant CaOx nucleation inhibition (**Figure 9, red**). In this case, EDTA is well known to complex Ca²⁺, thus this is EDTA decreasing the Ca²⁺ activity thereby leading to a lower supersaturation and lower nucleation kinetics. The morphology results, however, suggest that EDTA does also impact growth through adsorption given the significant change in morphology. EDTA inhibited nucleation in SUM but in the presence of zinc ions shows a nucleation behaviour similar to the control in SUM. The impact of EDTA in the presence of zinc ions can be easily and readily understood. The EDTA complexes preferentially with the zinc ions (Table 4) and releases Ca²⁺ so as to nucleate as per the control in SUM.

Zeta Potential:

In pure water, the zeta potential of the COM was found to be ~-12 mV and this became more positive on addition of zinc ions to ~-7mV (**SupFig 6**). The COM formed within SUM shows a zeta potential of -6.1±0.39 mV suggesting that the surface of the COM may have exposed negative groups, presumably oxalate ions (**Figure 10, black**). This value is more positive than that found in water as would be expected from an increase in ionic strength. However, when the zinc ions were incorporated into the solution the zeta potential of the particles becomes more negative to a value of -9.5±1.3 mV. One explanation of this decrease in the zeta potential could be attributed to an increased citric acid adsorption onto the surface of the COM. Previous studies carried out on the interaction of CA and COM has shown that the presence of CA in the growth solution results in a decrease of the zeta potential.[22] However, this was not observed in the pure water results (see **SupFig 6**) nor in our SUM data. It is hypothesised that CA is in fact complexing with Zn²⁺ ions and that this makes the zeta potential more negative because oxalate ions are exposed as opposed to their charges being screened by interacting with Zn²⁺ ions.

The COM grown in the presence of TA, or TA + Zn²⁺ in SUM shows no significant change in the zeta potential when compared to SUM alone, -6.3±1.8 and -6.27±1.0 respectively (**Figure 10, green**). This suggests that TA does not impact the double layer significantly, even when zinc ions are present at least in SUM. This is in sharp contrast to pure water+TA where addition of zinc ions resulted in a more positive zeta potential value (see **SupFig 6**). However, this does support the similar impact on nucleation behaviour irrespective of whether zinc ions are present in SUM as seen from the DLS results. The zeta potential of COM particles in SUM and the presence of MA show (both in the presence and absence of zinc ions) a value close to zero. The double layer is significantly impacted by MA and zinc ions do not impact significantly (**Figure 10, purple**). In pure water, the presence of MA showed COM particles had a zeta potential similar to the control COM particles (~-9.5±1.3 mV) but addition of zinc ions showed a positive zeta potential value (see **SupFig 6**). The presence of MA in SUM leads to a positive zeta potential and this supports the notion that MA is interacting with CA in the SUM. On addition of zinc ions a more negative zeta potential on COM particles is seen when MA is present in SUM. This is due to interaction of CA with zinc ions as discussed above for COM in SUM. In the case of EDTA, the formed COM particles have a zeta potential similar to the control COM, -7.1±2.4, in SUM but the addition of zinc ions results in particles with a more positive zeta potential, -1.4±0.5 (**Figure 10, red**). It would be expected that the EDTA should complex the zinc ions preferentially (Table 4) – so it might be expected that the zeta potential should be more negative (less screening of surface oxalate molecules). However, this is not

observed. Finally, for all these COM particles the value of the zeta potential implies that coagulation of the particles can occur and that aggregation of the particles is highly likely.

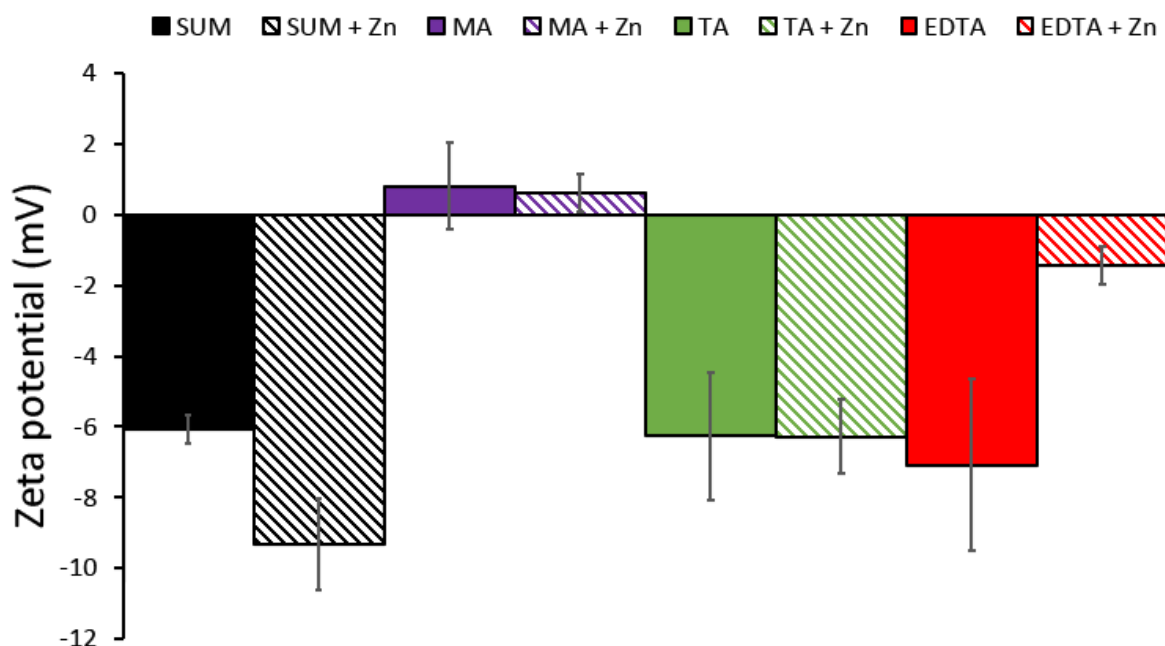


Figure 10) Comparison of the zeta potential of COM grown with (dashed) and without (solid) zinc ions and the respected organic.

Conclusions

In conclusion, in this manuscript the impact of various organic molecules in a more realistic solution medium is presented. The SUM used here has phosphate, citric acid and a buffered pH more comparable to real situations. The impact of SUM is to form rather flat, rounded particles that are typically seen in the presence of citric acid, the dominant SUM component. In the presence of zinc ions, the particles are little changed with the main change being more rounded particles.

The presence of the different organic acids show variability in their impacts depending on what interactions are occurring. The easiest of these to explain is that of EDTA. EDTA is a strong complexing agent that binds calcium ions, lowers the supersaturation and so inhibits nucleation. It also impacts the growing crystal leading to ‘rice’ shaped particles. On addition of zinc ions, however, the EDTA will preferentially complex Zn^{2+} ions so the supersaturation is increased back to the original SUM value resulting in particles that have the same morphology and nucleation behaviour as those in SUM alone. In the case of TA, the impact is one of a threshold inhibitor (meaning that TA is impacting nucleation and growth at very low levels[36]). Adsorption onto critical nuclei and/or growth features limits nucleation and growth. When zinc ions are present there is little impact on nucleation but the fact that the particles are more like COM grown in SUM (without zinc ions present) suggests that the impact may be similar on different faces.

Finally, the most complex behaviour is observed in the case of MA. It appears that MA interacts with CA in SUM leading to COM particles similar to that in pure water. This is seen by higher nucleation rates and a positive zeta potential of COM when MA is present in SUM. On addition of zinc ions the behaviour changes. The morphology of COM is the same as that of COM in SUM alone but the nucleation behaviour is significantly different in that it is significantly

inhibited. Thus, MA impacts nucleation more than growth when zinc ions are present. Despite these differences, the impact on zeta potential in the presence of zinc ions is only small.

For all of these organic molecules in the absence or presence of zinc ions, the zeta potential is quite small (absolute value is <10 mV) suggesting aggregation/agglomeration will be favoured. This in turn would promote larger stone formation.

In this work, it has been shown that while additives can impact by conventional means (e.g. like TA) as threshold inhibitors or as chelators, when a complex medium is used an additive can have a more complicated impact that has competing interactions with other species present in the medium (e.g. MA). As such all additives need to be thoroughly assessed in an environment that matches the actual environment it will be used in as closely as possible. As such, the next step for this work will be to investigate these promising additives in a medium that more closely matches real urine.

Acknowledgements

We would like to thank and acknowledge the John de Laeter Centre, Curtin University as a part of this research was undertaken using the EM instrumentation (ARC LE0775553). We would also like to acknowledge the Australian government for funding via the Australian postgraduate award and Curtin University for its use of facilities and equipment.

References

- [1] M.J. Nicar, K. Hill, C.Y.C. Pak, Inhibition by citrate of spontaneous precipitation of calcium oxalate in vitro, *J. Bone Miner. Res.* 2 (1987) 215–220.
- [2] S. Weiner, L. Addadi, Crystallization pathways in biomineralization, *Annu. Rev. Mater. Res.* 41 (2011) 21–40. <https://doi.org/10.1146/annurev-matsci-062910-095803>.
- [3] J. Aizenberg, S. Weiner, L. Addadi, Coexistence of Amorphous and Crystalline Calcium Carbonate in Skeletal Tissues, *Connect. Tissue Res.* 44 (2003) 20–25. <https://doi.org/10.1080/03008200390152034>.
- [4] J. Tao, D. Zhou, Z. Zhang, X. Xu, R. Tang, Magnesium-aspartate-based crystallization switch inspired from shell molt of crustacean, *PANS.* 106 (2009) 22096–22101.
- [5] R. Lakshminarayanan, R.M. Kini, S. Valiyaveetil, Investigation of the role of ansocalcin in the biomineralization in goose eggshell matrix, *PANS.* 99 (2002) 5155–5159.
- [6] G.J. Vermeij, The oyster enigma variations : a hypothesis of microbial calcification, *Cambridge Univ. Press.* 40 (2014) 1–13. <https://doi.org/10.1666/13002>.
- [7] M. Cusack, A. Freer, Biomineralization : Elemental and Organic Influence in Carbonate Systems, *Chem. Rev.* 108 (2008) 4433–4454.
- [8] V.R. Franceschi, H.T. Horner, Calcium oxalate crystals in plants, *Bot. Rev.* 46 (1980) 361–427. <https://doi.org/10.1007/BF02860532>.
- [9] T.A. Kostman, V.R. Franceschi, Cell and calcium oxalate crystal growth is coordinated to achieve high-capacity calcium regulation in plants, *Protoplasma.* 214 (2000) 166–179. <https://doi.org/10.1007/BF01279061>.
- [10] W.O.S. Doherty, Effect of Calcium and Magnesium Ions on Calcium Oxalate Formation in Sugar Solutions, *Ind. Eng. Chem. Res.* 45 (2006) 642–647. <https://doi.org/10.1021/ie0509037>.
- [11] O.A. GOLOVANOVA, Y.O. PUNIN, A.S. VYSOTSKIY, and V.R. KHANNANOV, Effect of Organic and Inorganic Impurities on the Nucleation of Calcium Oxalate Monohydrate, *Chem. Sustain. Dev.* 19 (2011) 463–470.

- [12] S. DEGANELLO, The Structure of Whewellite, $\text{CaC}_2\text{O}_4 \cdot \text{H}_2\text{O}$, at 328K, *Acta Crystallogr.* 2 (1981) 826–829.
- [13] A.J. Anjos, P. Nolasco, J.M.A. Marques, F. Cabrita, M.F.C. Pereira, A.P.A. De, On oral calcifications : sialoliths , dental calculi and tonsilloliths, *Microsc. Soc. Am.* 19 (2013) 23–24. <https://doi.org/10.1017/S1431927613000731>.
- [14] F.L. Coe, A. Evan, E. Worcester, Kidney stone disease, *J. Clin. Invest.* 115 (2005) 2598–2608. <https://doi.org/10.1172/JCI26662.2598>.
- [15] M.C. Chauvet, R.L. Ryall, Intracrystalline proteins and calcium oxalate crystal degradation in MDCK II cells, *J. Struct. Biol.* 151 (2005) 12–17. <https://doi.org/10.1016/j.jsb.2005.04.005>.
- [16] C.D. Scales, A.C. Smith, J.M. Hanley, C.S. Saigal, Prevalence of Kidney Stones in the United States, *Eur. Urol.* 62 (2012) 160–165.
- [17] L.H. SMITH, THE MANY ROLES OF OXALATE IN NATURE, *Trans. Am. Clin. Climatol. Assoc.* 113 (2002) 1–20.
- [18] A.P. Evan, Physiopathology and etiology of stone formation in the kidney and the urinary tract, *Pediatr. Nephrol.* 25 (2010) 831–841. <https://doi.org/10.1007/s00467-009-1116-y>.
- [19] S. Farmanesh, J. Chung, D. Chandra, R.D. Sosa, P. Karande, J.D. Rimer, High-throughput platform for design and screening of peptides as inhibitors of calcium oxalate monohydrate crystallization, *J. Cryst. Growth.* 373 (2013) 13–19. <https://doi.org/10.1016/j.jcrysgro.2012.09.018>.
- [20] J.L. Meyer, W.C. Thomas Jr., Trace Metal-Citric Acid Complexes as Inhibitors of Calcification and Crystal Growth: II. Effects of Fe(III), Cr(III) and Al(III) Complexes on Calcium Oxalate Crystal Growth, *J. Urol.* 128 (1982) 1376–1378.
- [21] J.A. Munoz, M. Valiente, Effects of trace metals on the inhibition of calcium oxalate crystallization, *Urol. Res.* 33 (2005) 267–272. <https://doi.org/10.1007/s00240-005-0468-4>.
- [22] T. Barker, M. Boon, F. Jones, The role of zinc ions in calcium oxalate monohydrate crystallization, *J. Cryst. Growth.* 546 (2020) 125777. <https://doi.org/10.1016/j.jcrysgro.2020.125777>.
- [23] S. Chutipongtanate, V. Thongboonkerd, Systematic comparisons of artificial urine formulas for in vitro cellular study, *Anal. Biochem.* 402 (2010) 110–112. <https://doi.org/10.1016/j.ab.2010.03.031>.
- [24] P. Brown, D. Ackermann, B. Finlayson, CALCIUM OXALATE DIHYDRATE (WEDDELLITE) PRECIPITATION, *J. Cryst. Growth.* 98 (1989) 285–292.
- [25] T.V.R.K. RAO, V.K. CHOUDHARY, Chemoinhibition of Mineralization of Urinary Stone Forming Minerals by Magnesium and Zinc Ions in Aqueous and Urinary Milieu, *Asian J. Chem.* 21 (2009) 1730–1738.
- [26] T. Ozgurtas, G. Yakut, M. Gulec, M. Serdar, T. Kutluay, Role of urinary zinc and copper on calcium oxalate stone formation, *Urol. Int.* 72 (2004) 233–236. <https://doi.org/10.1159/000077122>.
- [27] M.B. McBride, M. Frenchmeyer, S.E. Kelch, L. Aristilde, Solubility , structure , and morphology in the co-precipitation of cadmium and zinc with calcium-oxalate, *J. Colloid Interface Sci.* 486 (2017) 309–315. <https://doi.org/10.1016/j.jcis.2016.09.079>.
- [28] A. Frey-Wyssling, Crystallography of the Two Hydrates of Crystalline Calcium Oxalate in Plants, *Am. J. Bot.* 68 (1981) 130. <https://doi.org/10.2307/2443000>.
- [29] A.M. Cody, R.D. Cody, Contact and penetration twinning of calcium oxalate monohydrate ($\text{CaC}_2\text{O}_4 \cdot \text{H}_2\text{O}$), *J. Cryst. Growth.* 83 (1987) 485–498. [https://doi.org/10.1016/0022-0248\(87\)90242-9](https://doi.org/10.1016/0022-0248(87)90242-9).
- [30] S.R. Qiu, A. Wierzbicki, C.A. Orme, A.M. Cody, J.R. Hoyer, G.H. Nancollas, S.

- Zepeda, J.J. De Yoreo, Molecular modulation of calcium oxalate crystallization by osteopontin and citrate, 101 (2004) 1811–1815.
- [31] H. Fleisch, Inhibitors and promoters of stone formation, *Kidney Int.* 13 (1978) 361–371. <https://doi.org/10.1038/ki.1978.54>.
- [32] D.B. Milne, W.K. Canfield, J.R. Mahalko, H.H. Sandsted, Effect of dietary zinc on whole body surface loss of zinc: impact on estimation of zinc retention by balance method, *Am. J. Clin. Nutr.* 38 (1983) 181–186. <https://doi.org/https://doi.org/10.1093/ajcn/38.2.181>.
- [33] H.H. Sandsted, W. Au, Chapter 47 - Zinc, in: G.F. Nordberg, B.A. Fowler, M. Nordberg, L.T. Friberg (Eds.), *Handb. Toxicol. Met.*, 1st ed., Elsevier Inc., 2007: pp. 925–947. <https://doi.org/https://doi.org/10.1016/B978-0-12-369413-3.X5052-6>.
- [34] E. Ruiz-agudo, A. Burgos-cara, H. Cölfen, C. Rodriguez-navarro, C. Ruiz-agudo, A. Ibañez-velasco, A non-classical view on calcium oxalate precipitation and the role of citrate, *Nat. Commun.* 8 (2017) 1–10. <https://doi.org/10.1038/s41467-017-00756-5>.
- [35] P.M. May, D. Rowland, K. Murray, E.F. May, Joint Expert Speciation System, (n.d.). http://jess.murdoch.edu.au/jess_home.htm.
- [36] K.G. Cooper, L.G. Hanlon, G.M. Smart, R.E. Talbot, The threshold scale inhibition phenomenon, *Desalination.* 31 (1979) 257–266.